ISSN: 2723-9535

Available online at www.HighTechJournal.org

HighTech and Innovation Journal

Vol. 5, No. 4, December, 2024

Seismic Optimization Design and Application of Civil Engineering Structures Integrated with Building Robot System Technology

Shaoxu Li [1*], Lisen Shen [1]

[1] *Department of Civil Engineering and Architecture, Shijiazhuang University of Applied Technology, Shijiazhuang, Hebei, 050081, China.*

Received 29 January 2024; Revised 06 November 2024; Accepted 12 November 2024; Published 01 December 2024

Abstract

Objective: The seismic data monitoring is important for resource distribution, capacity planning, quality of service analysis, error monitoring and isolation, and safety management. The seismic optimization of building civil engineering structures is effectively improved. Several issues pertaining to seismic optimization monitoring of civil engineering structures have come to light as a result of the ongoing advancements in science, technology, and the internet. *Method*: The study creates a seismic optimization method for civil engineering structures, identifying hidden hazards and implementing safety management and control based on internet-based characteristics. Regarding the problem that the existing high-rise building installation projects mainly rely on manual work, the relevant technical research on the corresponding intelligent operation equipment for the installation project is carried out, the kinematics analysis of the construction installation robot is performed, and the search for security loopholes is realized under the seismic optimization design method of integrated building civil engineering structures to quickly find the safety adaptability. *Results*: The optimal safety weights and thresholds are obtained, and random initial thresholds and weights are used for seismic optimization of civil engineering structures for safety monitoring. This paper studies the seismic resistance of the current buildings and explains the seismic problems in civil engineering structures in detail while giving a feasible plan to eliminate potential safety hazards and avoid harm caused by earthquakes.

Keywords: Civil Engineering Structure; Earthquake Resistance; Building Robot System Technology; Seismic Optimization.

1. Introduction

Building safety and resistance against seismic occurrences are increasingly dependent on seismic optimization design in civil engineering constructions. The process of creating civil engineering structures that are resistant to seismic pressures involves a thorough method known as seismic optimization development and application for constructing civil engineered buildings incorporating building robot system technology [1]. It entails the use of modern components, innovative structural designs, and the development of robot systems for real-time monitoring. By integrating these developments, structures in seismically exposed places would perform greater overall, have a smaller impact following seismic events, and have optimal structural stability [2]. The use of innovative engineering, construction, and upkeep techniques and tools made possible by construction robot system technology further improves optimization. Buildings that can endure seismic pressures while avoiding damage and guaranteeing occupant safety constitute the heart of the seismic optimization design approach [3].

Multiple factors, including building supplies, structural arrangements, and dynamic response analysis, are taken into consideration in a thorough and complete manner. The use of building robot systems technology, which provides

* Corresponding author: 2015225010130@stu.scu.edu.cn

http://dx.doi.org/10.28991/HIJ-2024-05-04-017

creative solutions for effective construction and continuous structural evaluation, is essential to the process [4]. Because of their sensors, controls, and sophisticated control systems, these robots can carry out responsibilities precisely and accurately. Using contemporary components with higher seismic performance is one of the most important parts of seismic optimization design [5]. To increase resilience despite sacrificing other technical criteria, these materials, such as alloys of steel and powerful concrete, are carefully chosen and incorporated with the structures of construction. Moreover, real-time performance and structural health monitoring are made possible by the incorporation of construction robot systems [6]. Engineers can evaluate the efficacy of design ideas and make well-informed decisions regarding potential modifications by using the data that these robots receive on structure behaviors during seismic occurrences. Building robot systems does more than simply construction and monitoring; these also make maintenance and upgrading easier [7]. These are trained in performing maintenance, strengthening, and inspection tasks, which increases the longevity of buildings and lowers the possibility of seismic damage.

A paradigm change in the area of civil engineering can be seen in the collaborative efforts between seismic optimization development and the construction of robot platform technologies [8]. Designing structures to satisfy legal requirements and then regularly monitoring and improving them for resistance to developing seismic hazards, provides a proactive strategy for seismic adaptability. The building robot platform technology and seismic optimization design together represent a major development in civil engineering that might lead to safer and more durable structures in seismically susceptible regions [9]. It represents a shift towards more intelligent, robust structures that can fit the needs of contemporary architecture while withstanding the effects of the elements. The emergence of a new global age of profitable, seismically resistant structures is anticipated as the method of construction [10]. The objective of the study is to create and use sophisticated construction robot system technology in seismic optimization approaches for civil engineering structure design. According to the development of resistance to earthquake construction methods, the requires to improve building resiliency, security, and effectiveness against seismic disasters.

2. Literature Review

The performance of the optimization techniques and the suggested model are the main topics of the study, which lacks structural modeling knowledge. The DE algorithm performed greater than its equivalent in the majority of the scenarios, according to the results. The model's performance in prediction situations is demonstrated by the results [11].The method involves estimating the variables of the building model using the optimization techniques Differential Evolution (DE) and Particle Swarm Optimization (PSO).The seismic design optimization of structures is summarized in the study, with an emphasis on typical issue types, optimization targets, and techniques of solving. Present deficiencies and a few unresolved issues that merit more investigation in subsequent studies are examined together with an analysis of recent and past advances [12]. There are several optimization issues that have been put forth for the processes of analysis and the creation of structures that can withstand seismic excitations, which are at an evolving stage. The importance of efficiency and sustainability in the Architecture, Engineering, and Construction (AEC) sector is first discussed in the report, along with the history of the evaluation project. Subsequently, pertinent articles are obtained and chosen, and these chosen pieces undergo a statistical examination [13].

The chosen articles are next examined with respect to the optimization goals and the temporal and geographical patterns they exhibit. The gathered was evaluated and discussed, covering the four main phases in the structural optimization process: structural analysis and simulation, formulation of optimization issues, optimization methodologies, and computational software and design platforms. The suggested process works well for determining the greatest designs under a particular set of restrictions. It is discovered that the Risk Category criteria work well for optimizing both variables and overall cost. The variety of performance objectives imposed on structures subjected to seismic ground motion is continually expanding because of the growing concern for resilience among engineers and other stakeholders. This emphasizes the necessity for multi-objective optimization in design [14]. The article presents an examination and contrast of optimization algorithms for dynamic topology, with a focus on frequency domain approaches.

A technique for optimizing dynamic topology termed sum of modal compliances (SMC) is described, which is based on approaches from seismic engineering research. Several eigenmodes are considered in order to minimize the building vibration for seismic excitement, it is represented by a response spectrum [15]. The method modifies seismic dynamic load variables between a sequence of topology optimization problems that are independent of the design, hence controlling design-dependent loads from inertial effects. The paper presents an optimization strategy for producing moment-resisting frames (MRFs) using nonlinear fluid viscous dampers (FVDs) in seismic design. The qualities of the building components and damping devices are optimized simultaneously while the most effective layout of structures is investigated, with no predetermined criteria. Finally, utilizing an effective gradient-based optimization strategy, the issue is restated in an infinitely differentiable form [16]. Taking into account ensembles of ground movements, responses to variables of interest are estimated using a probabilistic method. The optimization criteria technique is adjusted generating finite element models of the structures, adding fictional strain energy, and employing a basic penalty methodology to take into account both material volume and displacement limitations at the same time. We examine the impact of shear wall-frame interactions for both connected and single shear walls. The definitions offer a useful method for identifying the crucial components of these constructions since gravity and seismic stresses affect the shear walls [17]. The findings offer fresh perspectives on where openings should be placed in structural and architectural engineering. The optimal outcomes of the suggested approach are confirmed using eight accelerograms of earthquakes that have been recorded, and the system is applied to real building structures. The differential evolution method (DEM) [18] based optimization is feasible, as evidenced by comparisons with the current methods. Assessing the seismic efficiency, the findings demonstrate a distinct pattern of increasing displacements with increasing importance values as a consequence, managed tuned mass dampers (TMD) exhibit an enhanced seismic performance.

3. Technology for Controlling Construction Robot

The main component of the building installation engineering system is the robot system, and its primary duties include grabbing, moving, positioning, and installing the glass curtains materials. For the sake of craftsmanship, each link in this six-degree-of-freedom robot is powered by an RV reducer and servo motor [19-20]. Figure 1 shows the flow of methodology.

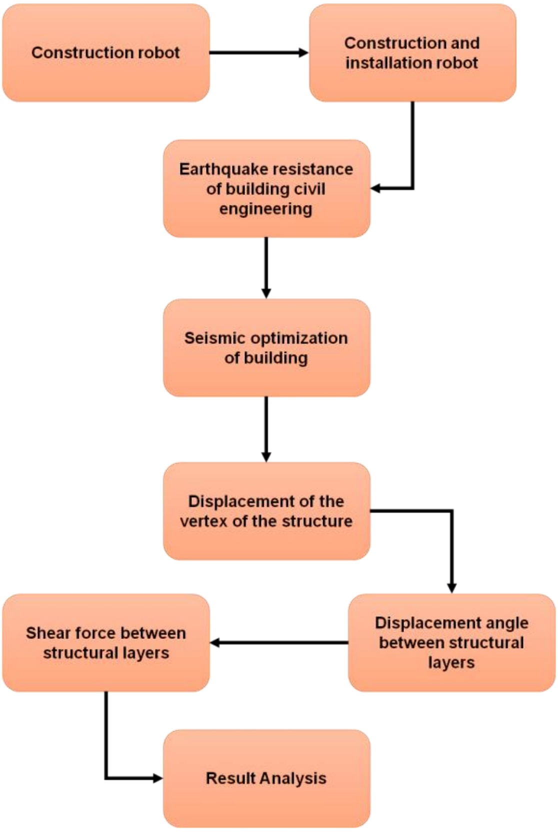

Figure 1. Flowchart of the methodology

The mechanical architecture of the robot is shown in Figure 2.

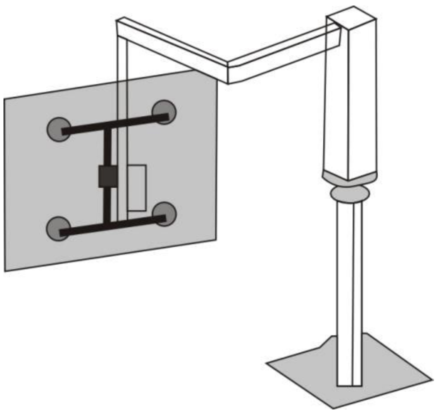

Figure 2. Architectural sketch of the robot used for building and installation

The robot terminal's schematic diagram is displayed in Figure 3.

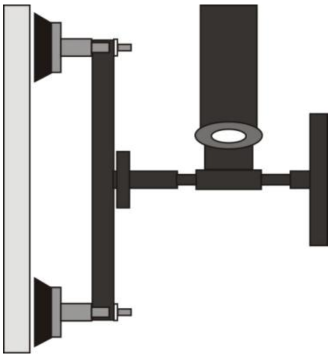

Figure 3. Schematic diagram of robot terminal and sensor installation

to fulfill the high-rise structures' glass curtains construction standards, on the original system for installing robots, the construction robot system is used in high-altitude operations. The architecture of the platform is shown in Figure 4.

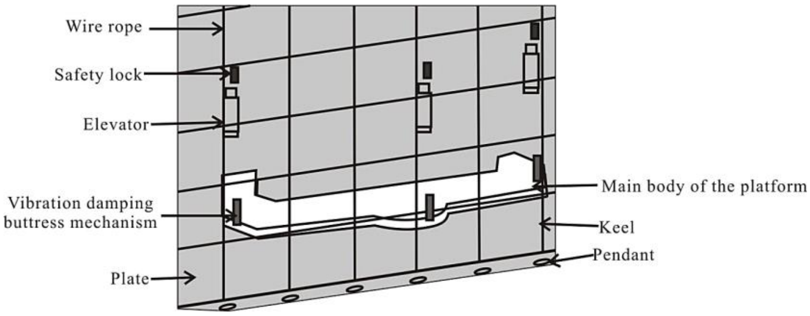

Figure 4. Gondola-type aerial work platform

According to the D-H rule, a coordinate system is established for the construction robot, as shown in Figure 5.

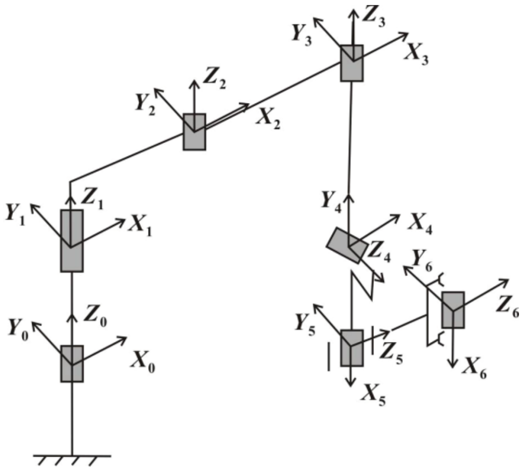

Figure 5. Joint coordinate diagram

Table 1. displays the joint variables and connecting rod characteristics.

Table 1. Connecting rod parameters and joint variable values

Joint i	α_i/(°)	α_{i-1}/ mm	d_i/mm	θ_i/(°)
1	0	0	d_1=1400	θ_1 (Variable)
2	0	a_2=1000	d_2(variable)	0
3	0	a_3=1000	0	θ_3 (Variable)
4	-90	0	d_4=1000	θ_4 (Variable)
5	-90	a_5=125	0	θ_5 (Variable)
6	0	0	d_6=210	θ_6 (Variable)

Based on the theoretical common sense of the D-H rule, the transformation matrix $A_n$between each coordinate system is calculated:

$$A_1 = Rot(z,\theta_1)Trans(0,0,d_1) = \begin{bmatrix} cos\,\theta_1 & -sin\,\theta_1 & 0 & 0 \\ sin\,\theta_1 & cos\,\theta_1 & 0 & 0 \\ 0 & 0 & 1 & d_1 \\ 0 & 0 & 0 & 1 \end{bmatrix} \tag{1}$$

$$A_2 = Trans(0,0,d_2)Trans(a_2,0,0) = \begin{bmatrix} 1 & 0 & 0 & a_2 \\ 0 & 1 & 0 & 0 \\ 0 & 0 & 1 & d_2 \\ 0 & 0 & 0 & 1 \end{bmatrix} \tag{2}$$

$$A_3 = Rot(z,\theta_3)Trans(a_3,0,0) = \begin{bmatrix} cos\,\theta_3 & -sin\,\theta_3 & 0 & a_3\,cos\,\theta_3 \\ sin\,\theta_3 & cos\,\theta_3 & 0 & a_3\,sin\,\theta_3 \\ 0 & 0 & 1 & 0 \\ 0 & 0 & 0 & 1 \end{bmatrix} \tag{3}$$

$$A_4 = Rot(z,\theta_4)Trans(0,0,d_4)Rot(x,90°) = \begin{bmatrix} cos\,\theta_4 & 0 & sin\,\theta_4 & 0 \\ sin\,\theta_4 & 0 & -cos\,\theta_4 & 0 \\ 0 & 1 & 0 & d_4 \\ 0 & 0 & 0 & 1 \end{bmatrix} \tag{4}$$

$$A_5 = Rot(z,\theta_5)Trans(a_5,0,0)Rot(x,-90°) = \begin{bmatrix} cos\,\theta_5 & 0 & -sin\,\theta_5 & a_5\,cos\,\theta_5 \\ sin\,\theta_5 & 0 & cos\,\theta_5 & a_5\,sin\,\theta_5 \\ 0 & -1 & 0 & 0 \\ 0 & 0 & 0 & 1 \end{bmatrix} \tag{5}$$

$$A_6 = Rot(z,\theta_6)Trans(0,0,d_6) = \begin{bmatrix} cos\,\theta_6 & -sin\,\theta_6 & 0 & 0 \\ sin\,\theta_6 & cos\,\theta_6 & 0 & 0 \\ 0 & 0 & 1 & d_6 \\ 0 & 0 & 0 & 1 \end{bmatrix} \tag{6}$$

Calculate the position matrix of the construction manipulator terminal by multiplying the above 6 transformation matrices:

$${}_6^0T = A_1A_2A_3A_4A_5A_6 = \begin{bmatrix} n_x & o_x & a_x & p_x \\ n_y & o_y & a_y & p_y \\ n_z & o_z & a_z & p_z \\ 0 & 0 & 0 & 1 \end{bmatrix} = [\vec{n} \quad \vec{o} \quad \vec{a} \quad \vec{p}] \tag{7}$$

Where:

$$n_x = \frac{1}{2}c_{134}c_{56} + s_{134}s_6 + \frac{1}{2}c_{5-6}c_{134} \tag{8}$$

$$n_y = \frac{1}{2}s_{134}c_{56} + c_{134}s_6 + \frac{1}{2}c_{5-6}s_{134} \tag{9}$$

$$n_z = c_6s_5 \tag{10}$$

$$o_x = \tfrac{1}{2}c_{5-6}c_{134} - \tfrac{1}{2}c_{134}c_{56} - s_{134}s_6 \tag{11}$$

$$o_y = \tfrac{1}{2}c_{5-6}s_{134} + c_{134}s_6 - \tfrac{1}{2}s_{134}c_{56} \tag{12}$$

$$o_z = -s_5s_6 \tag{13}$$

$$a_x = -c_{134}s_5 \tag{14}$$

$$a_y = -s_{134}s_5 \tag{15}$$

$$a_z = c_5 \tag{16}$$

$$p_x = a_3c_{13} + a_2c_1 + a_5c_{134}c_5 - d_6c_{134}s_5 \tag{17}$$

$$p_y = a_3c_{13} + a_2s_1 + a_5c_{134}c_5 - d_6s_{134}s_5 \tag{18}$$

$$p_z = d_1 + d_2 + d_4 + d_6c_5 + d_5s_5 \tag{19}$$

where s_i indicates $sin\,\theta_i$,c_i indicates $cos\,\theta_i$; s_{ij}indicates $sin(\theta_i + \theta_j)$, c_{ij}indicates $cos(\theta_i + \theta_j)$, s_{i-j} indicates $sin(\theta_i - \theta_j)$, c_{i-j} indicates $cos(\theta_i - \theta_j)$; s_{ijk}indicates $sin(\theta_i + \theta_j + \theta_k)$, c_{ijk} indicates $cos(\theta_i + \theta_j + \theta_k)$.

3.1. Inverse Solution of Kinematics of Construction and Installation Robot

Inverse kinematics analysis is relatively common in life and is the basis for the trajectory control and route planning of robots [21]. When starting the motion control of the robot, the variables of each joint of the robot should be calculated according to the target orientation and shape of the terminal, which is the inverse kinematics solution. Because the kinematics equation is a nonlinear equation system, it is very difficult to set up a robot inverse solution calculation method that can be used. Therefore, the methods for calculating the inverse solution of robot kinematics can be roughly divided into numerical methods, geometric methods, and algebraic methods [22].

By comparison, the inverse calculation of robot kinematics using Paul inverse transformation is the simplest method, and its calculation steps are as follows:

- Set up the kinematics equation of the robot ${}^0_6T = A_1A_2A_3A_4A_5A_6$;
- Using the $(A_1)^{-1}$left-handed multiplication kinematic equation, calculate $(A_1)^{-1}{}^0_TT = A_2A_3A_4A_5A_6$and solve the joint variable 1;
- Using the inverse matrix left-handed multiplication kinematics equation of the robot, the variables of each joint are calculated by the addition, multiplication, and trigonometric substitution of the matrix many times.

The expected location for the initial installation of the robot is:

$${}^0_6T = \begin{bmatrix} n_x & o_x & a_x & p_x \\ n_y & o_y & a_y & p_y \\ n_z & o_z & a_z & p_z \\ 0 & 0 & 0 & 1 \end{bmatrix} \tag{20}$$

Computing the inverse of each transformation matrix yields:

$$A_1^{-1} = \begin{bmatrix} c_1 & s_1 & 0 & 0 \\ -s_1 & c_1 & 0 & 0 \\ 0 & 0 & 1 & -d_1 \\ 0 & 0 & 0 & 1 \end{bmatrix}, A_2^{-1} = \begin{bmatrix} 1 & 0 & 0 & -a_2 \\ 0 & 1 & 0 & 0 \\ 0 & 0 & 1 & -d_2 \\ 0 & 0 & 0 & 1 \end{bmatrix}, A_3^{-1} = \begin{bmatrix} c_3 & s_3 & 0 & -a_3 \\ -s_3 & c_3 & 0 & 0 \\ 0 & 0 & 1 & 0 \\ 0 & 0 & 0 & 1 \end{bmatrix}, A_4^{-1} = \begin{bmatrix} c_4 & s_4 & 0 & 0 \\ 0 & 0 & 1 & -d_4 \\ s_4 & -c_4 & 0 & 0 \\ 0 & 0 & 0 & 1 \end{bmatrix},$$

$$A_5^{-1} = \begin{bmatrix} c_5 & s_5 & 0 & -a_5 \\ 0 & 0 & -1 & 0 \\ -s_5 & c_5 & 0 & 0 \\ 0 & 0 & 0 & 1 \end{bmatrix}, A_6^{-1} = \begin{bmatrix} c_6 & s_6 & 0 & 0 \\ -s_6 & c_6 & 0 & 0 \\ 0 & 0 & 1 & -d_6 \\ 0 & 0 & 0 & 1 \end{bmatrix},$$

Because joints 2 3 and 4 are parallel to each other, the following is calculated by the $(A_1)^{-1}$left-handed multiplication kinematics equation and$(A_6)^{-1}(A_5)^{-1}$ right-multiplication kinematics equation:

$$(A_1)^{-1}T_6^0(A_6)^{-1}(A_5)^{-1} = A_2A_3A_4 = A_{24} \tag{21}$$

So, calculate:

$$\begin{bmatrix} c_1 & s_1 & 0 & 0 \\ -s_1 & c_1 & 0 & 0 \\ 0 & 0 & 1 & -d_1 \\ 0 & 0 & 0 & 1 \end{bmatrix} \begin{bmatrix} n_x & o_x & a_x & p_x \\ n_y & o_y & a_y & p_y \\ n_z & o_z & a_z & p_z \\ 0 & 0 & 0 & 1 \end{bmatrix} \begin{bmatrix} c_6 & s_6 & 0 & 0 \\ -s_6 & c_6 & 0 & 0 \\ 0 & 0 & 1 & -d_6 \\ 0 & 0 & 0 & 1 \end{bmatrix} \begin{bmatrix} c_5 & s_5 & 0 & -a_5 \\ 0 & 0 & -1 & 0 \\ -s_5 & c_5 & 0 & 0 \\ 0 & 0 & 0 & 1 \end{bmatrix} = A_{24} \tag{22}$$

The formula's third columns and row's components are equal, to get:$o_zc_6 + n_zs_6 = 0$

Calculated in one step:$\theta_6 = -\,arctan\frac{o_z}{n_z}$

In the formula, the components of the primary column and the last row are equal to calculate:$p_z - d_1 - a_zd_6 - a_5(n_zc_6 - o_zs_6) = d_2 + d_4$

Calculated in one step: $d_2 = p_z - d_1 - a_z d_6 - a_5(n_z c_6 - o_z s_6) - d_4$

Based on the $(A_1)^{-1}$ left-handed multiplication kinematics equation and the $(A_6)^{-1}(A_5)^{-1}(A_4)^{-1}$ right-multiplication kinematics equation, get:

$$\begin{bmatrix} c_1 & s_1 & 0 & 0 \\ -s_1 & c_1 & 0 & 0 \\ 0 & 0 & 1 & -d_1 \\ 0 & 0 & 0 & 1 \end{bmatrix} \begin{bmatrix} n_x & o_x & a_x & p_x \\ n_y & o_y & a_y & p_y \\ n_z & o_z & a_z & p_z \\ 0 & 0 & 0 & 1 \end{bmatrix} \begin{bmatrix} c_6 & s_6 & 0 & 0 \\ -s_6 & c_6 & 0 & 0 \\ 0 & 0 & 1 & -d_6 \\ 0 & 0 & 0 & 1 \end{bmatrix} \begin{bmatrix} c_5 & s_5 & 0 & -a_5 \\ 0 & 0 & -1 & 0 \\ -s_5 & c_5 & 0 & 0 \\ 0 & 0 & 0 & 1 \end{bmatrix} \begin{bmatrix} c_4 & s_4 & 0 & 0 \\ 0 & 0 & 1 & -d_4 \\ s_4 & -c_4 & 0 & 0 \\ 0 & 0 & 0 & 1 \end{bmatrix} = A_{23} \tag{23}$$

The components of the formula's second column and third row are identical to calculate:

$$c_4\big(a_z s_5 - c_5(n_z c_6 - o_z s_6)\big) - s_4(o_z c_6 + n_z s_6) = 0 \tag{24}$$

Calculated in one step:

$$\theta_4 = arctan\frac{a_z s_5 - c_5(n_z c_6 - o_z s_6)}{o_z c_6 + n_z s_6} \tag{25}$$

Based on the $(A_6)^{-1}(A_5)^{-1}(A_4)^{-1}$ right multiplication kinematic equation, obtain:

$$\begin{bmatrix} n_x & o_x & a_x & p_x \\ n_y & o_y & a_y & p_y \\ n_z & o_z & a_z & p_z \\ 0 & 0 & 0 & 1 \end{bmatrix} \begin{bmatrix} c_6 & s_6 & 0 & 0 \\ -s_6 & c_6 & 0 & 0 \\ 0 & 0 & 1 & -d_6 \\ 0 & 0 & 0 & 1 \end{bmatrix} \begin{bmatrix} c_5 & s_5 & 0 & -a_5 \\ 0 & 0 & -1 & 0 \\ -s_5 & c_5 & 0 & 0 \\ 0 & 0 & 0 & 1 \end{bmatrix} \begin{bmatrix} c_4 & s_4 & 0 & 0 \\ 0 & 0 & 1 & -d_4 \\ s_4 & -c_4 & 0 & 0 \\ 0 & 0 & 0 & 1 \end{bmatrix} = A_{13} \tag{26}$$

In the formula, the elements in the first row and the fourth column are equal to calculate:

$$c_{13} = -c_4[a_z s_5 - c_5(n_z c_6 - o_z s_6)] - s_4(o_z c_6 + n_z s_6) \tag{27}$$

Combining the above two formulas, the following can be calculated:

$$a_3 c_{13} + a_2 c_1 = p_x - a_x d_6 - a_5(n_x c_6 - o_x s_6) - d_4[a_x c_5 + s_5(n_x c_6 - o_x s_6)] \tag{28}$$

Combining the above two formulas, the following can be calculated:

$$\theta_1 + \theta_3 = arccos[c_4 a_x s_5 - c_4 c_5(n_x c_6 - o_x s_6) + s_4(o_x c_6 + n_x s_6)] \tag{29}$$

$$\theta_1 = arccos\frac{p_x - a_x d_6 - a_5(n_x c_6 - o_x s_6) - d_4[a_x c_5 + s_5(n_x c_6 - o_x c_6)] - a_3 c_{13}}{a_2} \tag{30}$$

This building assembly robot does not exceed eight sets of solutions. Some of the solutions are inconsistent with the actual situation due to the limitation of the joint activity area. Except for the partial solution, the remaining solutions are to choose the best solution according to the shortest travel rule. The movement of each joint must be minimized. Because this robot is a serial robot, it is suitable to use the weighted method to handle it, which meets the requirement of "moving small joints more frequently than large joints".

3.2. Analysis of the Main Factors of Earthquake Resistance in Building Civil Engineering

3.2.1. Traditional Seismic Method

First of all, the traditional seismic concept is summed up from long-term construction experience, and there is no precise measurement and objectivity. It is obtained subjectively and partly objectively. In addition, even if the results of analysis and calculation are carried out at an objective level, such results are qualitative rather than quantitative. The design of seismic buildings conceptually imposes overload, which imposes certain constraints on the work of designers of building balances.

3.2.2. Fundamentals of Structural Design

In order to increase the service life of the seismic optimization of building civil engineering structures as much as possible, and reduce the packet loss and time delay in the transmission process of seismic optimization data information of building civil engineering structures, it is necessary to carry out topology and optimization of the structure for seismic optimization of building civil engineering structures. Based on the real-time monitoring platform for seismic optimization of building civil engineering structures, a real-time monitoring method for seismic optimization of building civil engineering structures is proposed, monitoring is performed according to the threshold value of the seismic optimization nodes of building civil engineering structures, and all monitoring links for seismic optimization of building civil engineering structures need to be balanced. Next is the design of the longitudinal structure, so that the distribution is even. Avoid the disturbance of the building by the influence of external force. Feasibility measures are added to the building design, focusing on the foundation design of the building. The load-bearing capacity of the ground floor is poor, which will cause each component to be weak and deviate from the center of gravity [23].

3.3. Seismic Optimization Design of Building Civil Engineering Structures

Connecting the boundaries to the different layers to form the final geological model, the input signal to the monitoring system can be expressed as:

$$x(t)=\sum_{n=1}^{M} U_n \, sin(n2\pi f_0 t+n2\pi \Delta f t+\theta_n)+U_0 \tag{31}$$

Consider only the fundamental component, and set $\theta(t)=2\pi\Delta ft+\theta 1$, then

$$\frac{d\theta(t)}{dt}=2\pi\Delta f \tag{32}$$

Using the value of conductivity is transformed using the discrete differential equation, and measured for a duration of the time step is $T_0 \ = \ 1/f_0$.

$$\Delta\theta=2\pi\Delta f\Delta t=2\pi\Delta fT_0=\frac{2\pi\Delta f}{f_0} \tag{33}$$

$$f=f_0+\Delta f=f_0+\frac{f_0\Delta\theta}{2\pi} \tag{34}$$

The procedure for measuring frequency. The elementary wave's optimal frequency is $f_0 \ = \ 100Hz$. The actual frequency of the power grid generally changes slowly around $f0$, so it is enough to calculate the phase deviation correctly. The actual frequency f can be determined.

According to the technical principle of the construction robot system, the real and imaginary parts can be obtained as:

$$a_n=\frac{2}{N}\sum_{k=0}^{N-1} x(k)\, cos\left(nk\frac{2\pi}{N}\right) \tag{35}$$

$$b_n=\frac{2}{N}\sum_{k=0}^{N-1} x(k)\, sin\left(nk\frac{2\pi}{N}\right) \tag{36}$$

In the formula: $N$is the quantity of interval sampling sites; $x(k)$ is sample data.

Related systems with multiple subgroups working together for evolution can be used to solve a number of problems related to the seismic optimization of buildings. The different subgroups can work together relatively independently, collaborating and interacting with each other using individual data to find the most appropriate solution to the problem. The improvement of the robotic system during the construction process is carried out in two different ways, side by side. On the one hand, a relatively external archive will be created to store the best solutions to the problems associated with construction robots. On the other hand, the diversity of the combinations will be improved to introduce the related strategy selected by the elite and to continuously update the external file with individual concave and convex problems. With the effective increase of the number of optimal problem solutions proposed for external files, the capacity of their storage increases, leading to inefficiencies in the system algorithm. an upper limit is specified for the specific external storage file for optimization problems related to the existence of multiple items in different groups. This is by far the best solution to the inefficiency problem. When the number of optimal solutions for the external storage files is full, the effective efficiency of the relevant algorithm is improved by using an overload distance policy to remove some optimal solutions that have exceeded the upper limit.

The maximum number hop of jumps of seismic learning factor sk is set. $count\_max\ (s,v)\ \chi_k$ is associated with the building civil engineering structure seismic optimization monitoring routing itself, and $Tag(k) \ = \ 0$.

$$\left|\frac{d(s_k,v_0)}{d_0}-\chi_k\right|\leq 0.5 \tag{32}$$

The best design for seismic-specific features throughout the building space is to take advantage of the seismic performance of the relevant structural features and to minimize the cost of construction, but there is a conflict between the seismic capacity of the relevant structural features and the lower cost of construction. The optimal solution to the problem is obtained by using a number of different subgroups for certain effective optimization methods and by using information data for shared calculations.

It is set to evolve between several groups, the goal of each specific optimization is to find the specific direction of interest within this grouping for the best solution to the problem, which is not only for the global optimal solution but is also influenced by some extent by the effective speed of individual pickups and the specific location of the pickups in other groups. A specific external file is set up to be shared, and the valid data related to the best solution to the problem obtained during the fast search is repeated among the construction machines in multiple groups and can be input from several different subgroups with a certain coordination and after optimization of the structure schematic, as shown in Figure 6.

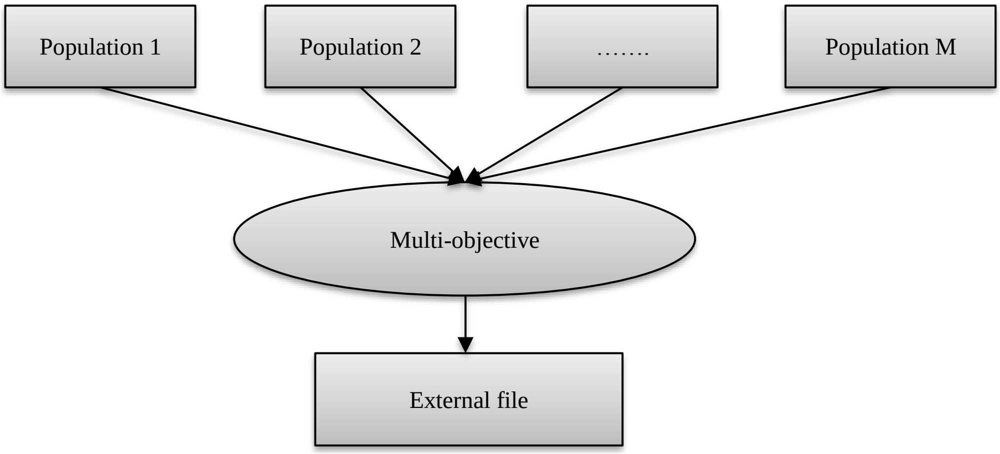

Figure 6. Structural diagram of collaborative optimization of multi-sub-robots

According to the structural diagram in Figure 1, the specific choice of values for automatic adaptation is determined by the M-s objective function. Multiple self-combining groups are used to optimize multiple specific objectives together. Each team combination selects the relevant intelligent robot for its own use in the building structure. These selected best intelligent robots exchange data and information in order to achieve the closest algorithm to the best solution to the problem.

In order to efficiently implement the exchange of data and information between different groups of people, external storage files are placed in the control process of the building intelligent robot system. This file can be set up to speed up the algorithm to a certain extent so that the data information moves quickly to the forefront of the best solution to the problem.

Through effective data calculation to obtain a series of automatically correlated functions ACF and polarization to carry out the autocorrelation function TACF, the specific order of the relevant model and the value of the parameter β can be determined through the operation of these two functions, and the following monitoring equation specific operation formula can be obtained.

$$G_0 = 1, G_i = \sum_{k=1}^{i} \left(\phi_k^{'} G_{i-k} - \theta_k^{'}\right) (k \geq 1) \tag{38}$$

$$\widehat{x}_t(l) = \begin{cases} \mu + \sum_{i=1}^{p} \phi_i \widehat{x}_t(l-i) - \sum_{i=l}^{q} \phi_i \varepsilon(t+l-i), l \leq q \\ \mu + \sum_{i=1}^{p} \phi_i \widehat{x}_t(l-i), l > q \end{cases} \tag{39}$$

$$Var\left(e_t(l)\right) = \sum_{i=0}^{l-1} G_i^2 \sigma_\varepsilon^2, \forall l \geq 1 \tag{40}$$

Where;

$$\phi_k^{'} = \begin{cases} \phi_k, 1 \leq k \leq p \\ 0, k > p \end{cases} \tag{41}$$

$$\phi_k^{'} = \begin{cases} \theta_k, 1 \leq k \leq q \\ 0, k > q \end{cases} \tag{42}$$

$$\hat{x}_t\,(k) = \begin{cases} \hat{x}_t\,(k), k \geq 1 \\ x_{t+k}, k \leq 0 \end{cases} \tag{43}$$

σ_ε^2 can be replaced by sample variance $\hat{\sigma}_\varepsilon^2$: here e_i is the discrepancy between the alert value that was using the 1-step alarm equation and the actual observation value.

$$\hat{\sigma}_\varepsilon^2 = \left(\sum_{i=1}^{t} \frac{(e_i - \overline{e})^2}{(t-1)}\right), \overline{e} = \sum_{i=1}^{t} \frac{e_i}{t} \tag{44}$$

Denote Pt as the monitoring value at time t obtained according to the construction robot system technology, let $\varepsilon = \lambda\sqrt{(1+\varphi_1^2+\cdots+\varphi_q^2)\sigma_\varepsilon^2}, \lambda > 1$, function as a stable, and it is probable that the interval $[P(t)-\varepsilon, P(t)+\varepsilon]$ lacks the actual worth at that moment$t$ is $\frac{1}{\varepsilon^2}$ at most.

3.4. The Relationship between the Shear Force at the Bottom and the Displacement of the Vertex of the Structure

Aiming at the problem of low accuracy of seismic optimization monitoring of current building civil engineering structures, this paper proposes a seismic optimization method for building civil engineering structures based on the construction robot system technology by using the weights and thresholds of the algorithm in this paper. The construction robot system technology is used to analyze the seismic optimization requirements of building civil engineering structures to construct a binary combinatorial optimization model based on the constraints related to the seismic optimization nodes and links of the civil engineering structure of the bottom building, which can effectively realize the basic mapping of the seismic optimization resources of the civil engineering structure of the bottom building, and can also reduce the cost and time spent on seismic optimization of the underlying building civil engineering structure, thereby improving the success rate, revenue and resource utilization rate of virtualized mapping of the seismic optimization of building civil engineering structure. Figure 7 justifies the improved horizontal force distribution method shown in this paper. Moreover, the more irregular the longitudinal arrangement of the structures, the greater the deviation from the uniform distribution and the inverse triangular distribution.

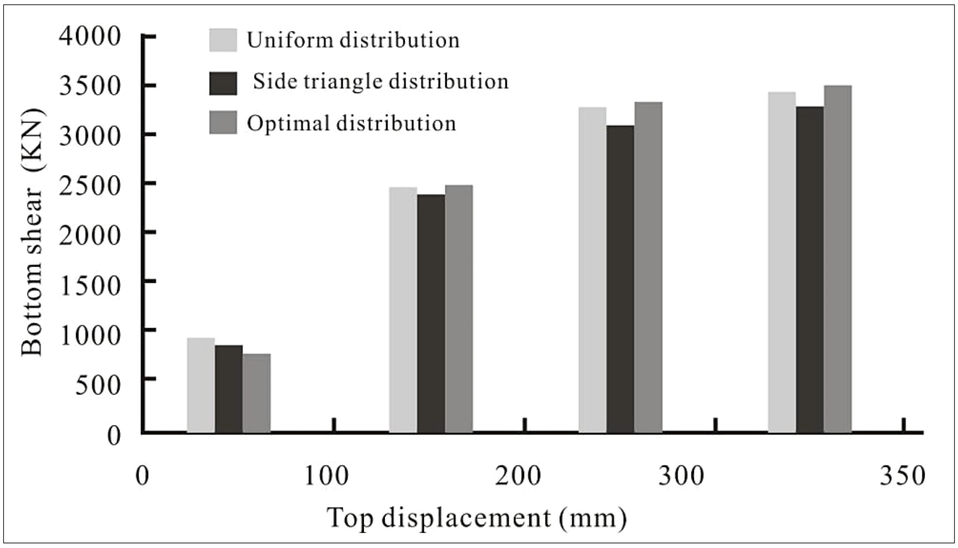

Figure 7. Displacement-bottom shear curve of structure vertex

3.5. Distribution and Deviation of Displacement Angle between Structural Layers

Distribution of displacement angle between layers of structure:

The extraction of the structure is the interlayer displacement angle of three levels of load distribution forms (uniform distribution, inverted triangular distribution, and optimal distribution). It can be seen from Figure 8 that the comparison between the interlayer displacement angle and time distribution obtained with the optimized lateral force distribution is similar, and the displacement angle changes more uniformly with height.

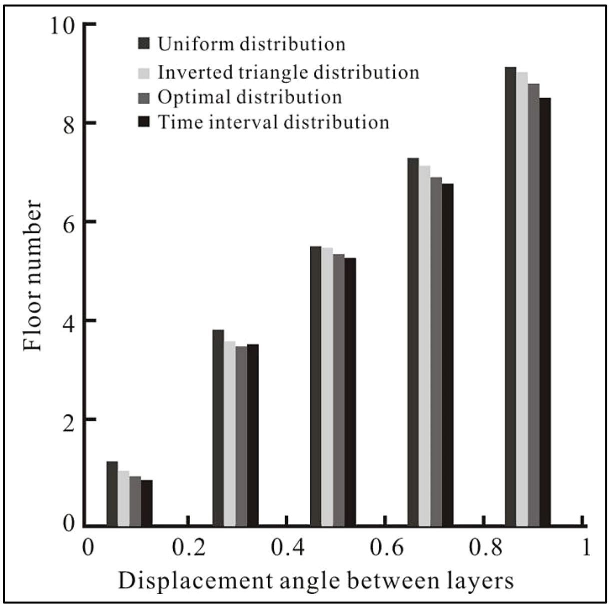

Figure 8. Dispersion of the displacement angle between the structural layers

The deviation E_i of the inter-story displacement angle of the i-th layer of the structure is defined as:

$$E_i = \frac{d_{pi} - \overline{d}_{Ti}}{\overline{d}_{tI}} \tag{44}$$

Among them, the average value $\overline{d}_{Ti}$ of the displacement angle between the ith layers of the d_{pi} structure is obtained from the distance analysis between the shear force and the dynamic force between the ith layers of the structure.

It can be seen from Figure 9 that there are three horizontal and lateral distribution forms of uniform distribution, optimal distribution, and inverted triangular distribution in the structural layer, and the difference between the displacement angles between the layers can be found. It can be calculated that the displacement angle difference of the lower layer can reach 36% in the case of uniform distribution. The resulting inverted triangular distribution of the graph obtained is also relatively scattered about 22%. The distribution can be changed so that the minimum deviation is about 10%. In addition, since the deviation of the change distribution is relatively small, it can be concluded that the lateral force of the seismic analysis by improving the structural energy has a significant effect.

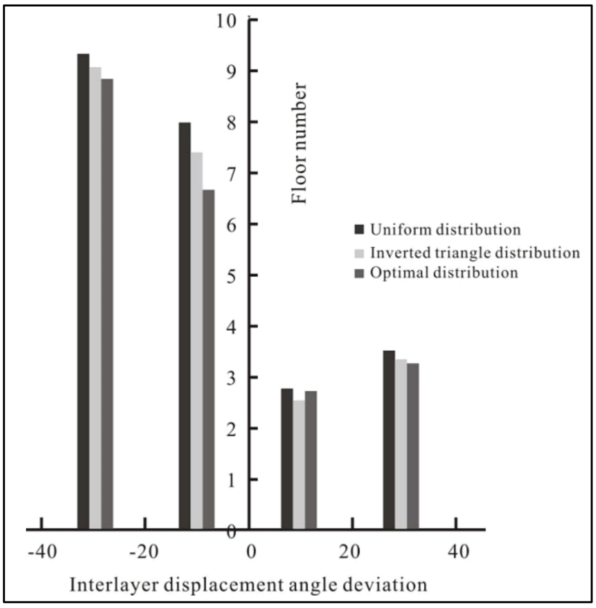

Figure 9. Displacement angle deviation between layers of structure

3.6. Distribution and Deviation of Shear Force Between Structural Layers

(1) Distribution of shear force between structural layers:

According to the test results in Figure 10, the distribution of shear force between layers of the structure can be represented by three horizontal load distributions. The obtained homogeneous distribution is quite different from that obtained from the inverse triangular distribution. By improving the distribution and time, the analytical results obtained are relatively similar, and in the meantime, the dynamic characteristics of the structure can be tested to a certain extent.

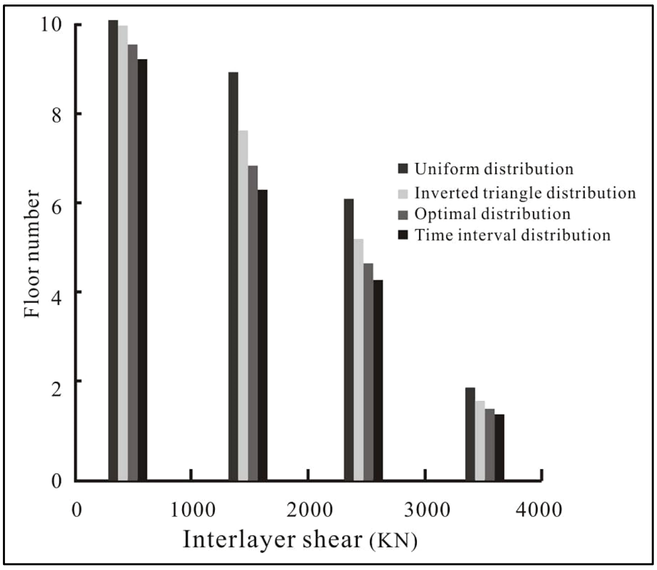

Figure 10. Distribution of shear force between structural layers

(2) Deviation of shear force between structural layers:

The deviation E_i of the interlayer shear force at the i^{th} layer of the structure is defined as:

$$E_i = \frac{V_{pi} - \overline{V}_{Ti}}{\overline{V}_{tI}} \tag{44}$$

In the expression, V_{pi} and $\overline{V}_{Ti}$ are used to represent the inter-story shear force and examination of dynamical time history correlating with the structure's i^{th} layer in turn, and the average value of the inter-story shear force corresponding to the i-th layer can be obtained.

Figure 11 shows that under three horizontal load distributions, the distribution of shear force deviation between different layers can be calculated, and the deviation value of interlayer shear force can be calculated under the average distribution, and the maximum value that can be reached is about 38%. The inverse triangular distribution has a relatively small deviation of about 35%. According to the test results, the distribution optimization effect of seismic shear force is obviously improved.

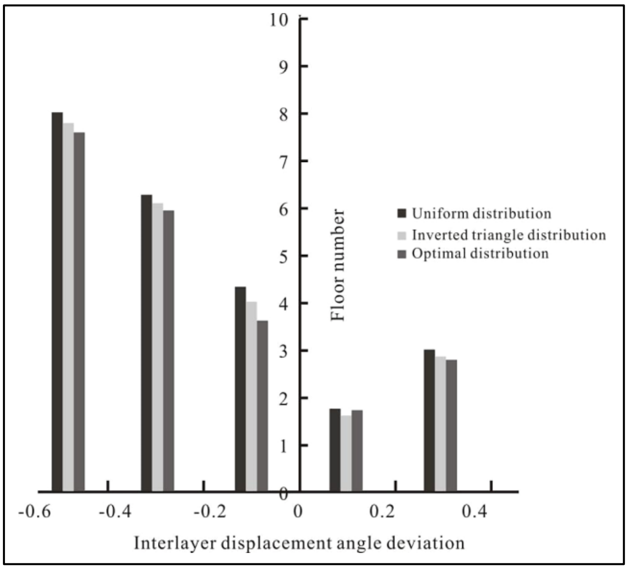

Figure 11. Shear force deviation between structural layers

4. Analysis of Experiment and Data

In order to effectively verify the degree of feasibility for the design at the practical operation level, a series of relevant experimental tests and effective analyses were conducted for the specific stability, excellent performance aspects, optimization cost perspective, and seismic performance aspects of the design method. The results of the tests are shown in Figure12, after nearly 20 iterations of optimization using the group optimization program created for the calculated examples. The structural content of Table 2 shows the design diagram and the optimization outcomes for the building's seismic performance following optimization. In G-PSO is used as a technically relevant representation of the construction robot system, C is used as a component group representing the presence of component J in the original design, K represents the optimal cost ($) obtained after the calculation, G is used as a specific representation of the relevant standard deviation ($), D is used as a representative value of the average number of runs (times), and P represents the effective number of analyses (times) of Purever. This involves assessing the results of using intelligent robots to optimize building architecture. The test findings evaluate how well this technology works to improve structural efficiency, possibly by evaluating variables such as cost reductions, increased durability, or faster construction to robotic interventions throughout the building process.

It can be seen that, in comparison with the ACO algorithm in the literature, the continuous improvement of the building structure intelligent robotics system technology has led to a series of effective improvements in the prediction of earthquakes and also to an effective reduction in the construction cost of buildings. By using the system technology related to intelligent robots for building structures, it was necessary to reach an optimal value after the third test, i.e., 57.9% of the predicted building design cost in the original design plan. The standard deviation results given by the calculations in Table 2 also show to some extent that the stability of the improved system technology related to intelligent robotics for building structures is relatively able to reach the ideal state.

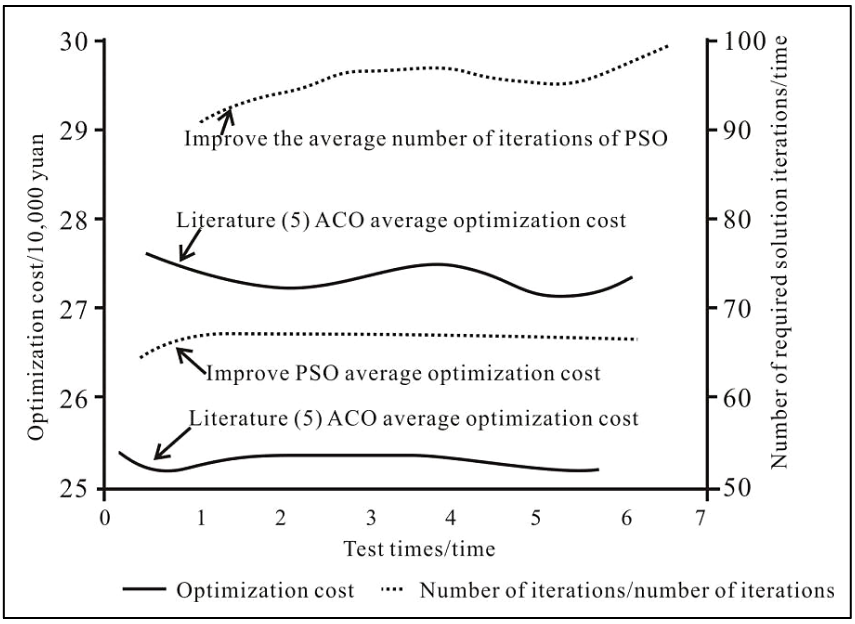

Figure 12. Test results for certain optimization of the building structure intelligent robotics system technology

Table 2. Results after optimization of system technologies related to intelligent robots for building structures

W	K/yuan	G/yuan	D / times	P / times
C	45210	-		
G-PSO	26210	741	135	854
NSGA-II	28654	789	70	4500
ACO	30254	1524	145	6452

The table displays comparative information on the performance metrics of optimization algorithms: The issue cases are K and G, and the execution times are shown by D and P. The algorithms C, G-PSO, NSGA-II, and ACO are represented by the corresponding rows. For example, NSGA-II demonstrated faster execution times (D) than ACO, even though ACO had marginally greater fitness values (G). This data suggests trade-offs between the efficacy (fitness) and efficiency (time) of algorithms, which are important factors to take into account when selecting an optimization strategy based on certain requirements like speed or quality of the solution.

For the building structure intelligent robot-related system technology, the ACO algorithm proposed in the literature [5] and the NSGA-II algorithm mentioned in the literature [6], these three different algorithms were compared in terms of the specific number of runs and the effective number of analyses for Pushover, and the specific comparative results obtained are shown in Figure 13. The smart robotics system technology for building structure optimization operation procedures makes use of sophisticated algorithms and sensors to improve productivity and performance during construction projects. This technology uses robotic capabilities to design evaluation, material handling, and assembly, which simplifies workflows, lowers mistakes, and enhances productivity.

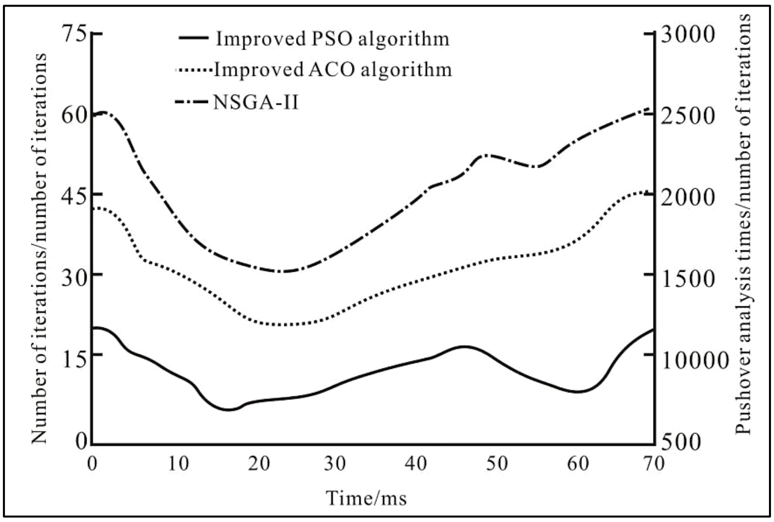

Figure 13. Optimization operation process

the comparison of the three optimization processes shows that the average number of runs of the technical algorithm of the intelligent robot-related system of the building structure after the improvement is 8, while the average number of runs obtained after the calculation of the algorithm of the ACO proposed by Chea et al. [5] is 28, and the NSGA-II algorithm applied by Leyva et al. [6] has the highest average number of runs, reaching 45. In terms of the number of effective analyses performed by Pushowver, the number of analyses performed by the algorithm designed to perform the scheduling associated with virtual augmented reality cluster centers in this paper is also the lowest, and this result largely represents the relatively low computational effort required for the scheduling algorithm associated with virtual augmented reality cluster centers. It also validates the advantageous feature of superior speed that we have been pursuing.

The structure given in Figure 14 shows to some extent the system technology related to intelligent robotics for building structures, the ACO algorithm proposed by Chea et al. [5], and the NSGA-II algorithm mentioned in the application by Leyva et al. [6], in the curve used to carry out the solution repetition, in order to compare and thus obtain an optimal and effective optimization result. The building structure intelligent automation system technological cost optimization curve shows how to strike a compromise between the initial expenditure of funds and the long-term savings realized from effective robotic systems. It indicates that overall cost savings result from a gradual drop in upfront expenses as efficiency, maintenance, and operational efficiency rise.

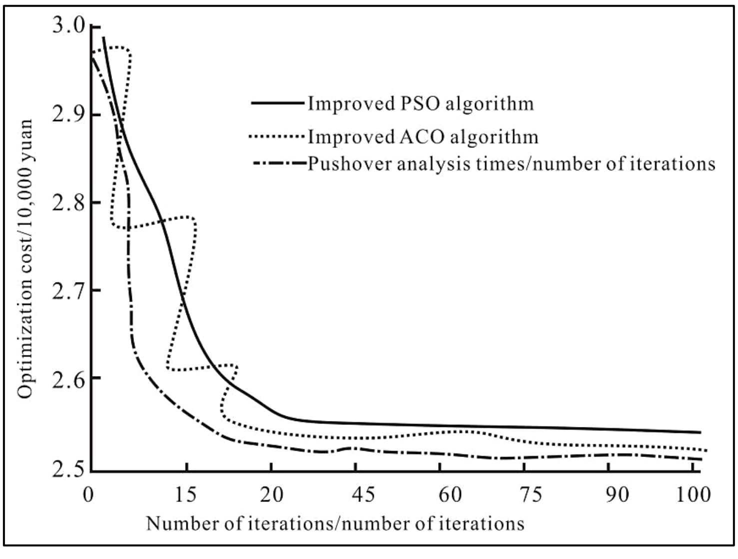

Figure 14. Cost optimization curve

As shown in the relevant results provided in Figure 13, the system technology used for intelligent robotics related to building structures updates individual files located in external storage files by using a certain elite selection strategy, which also reduces the optimization cost from $29,800 to $2,520 before performing 30 operations, a reduction of 15.7%, which can be used to some extent as a representation of the optimal solution. This can also show to a certain extent that the technology of intelligent robotic systems for building structures can effectively save the seismic capacity of the building site, thus effectively saving the design costs of optimized buildings and playing a very positive role in achieving efficiency and reducing optimization costs.

The results in Table 3 also show the specific seismic performance status of the building structure after certain optimization of the system technology for building structure intelligence robotics.

Table 3. Comparison of seismic performance correlation of different algorithms for the results after performing optimization

Algorithm	Top layer displacement/cm		Interlayer displacement angle/%	
	AC	BK	AC	BK
Performance requirements	4.85	6.25	125	6.00
Improved PSO algorithm	3.58	4.24	0.65	3.58
Improved ACO algorithm	4.25	7.25	0.89	4.25
NSGA - II algorithm	4.35	7.85	0.88	5.27

The displacement data and interlayer displacement angles for several algorithms, such as AC, BK, Enhanced PSO, Improved ACO, and NSGA-II, are shown in this table. The performance standards include that the displacement for AC and BK should be 4.85 cm and 6.25 cm, respectively, with interlayer movement angles of 6.00% for BK and 125% for AC. An angle of 0.65% and an excursion of 3.58 cm are obtained by the Improved PSO method. The 4.25 cm and 7.25 cm displacements and 0.89% and 4.25% angles, respectively, are displayed using the Improved ACO algorithm. The NSGA-II algorithm displays 4.35 cm and 7.85 cm displacements together with 0.88% and 5.27% angles. The comparative results of seismic performance that can be expressed by different performance algorithms in Table 3 show that the data of top layer displacement values and interlayer displacement angles of the improved building structural intelligence-related calculation method for each different performance mode requirement are within the maximum range and are lower than the results of the two algorithms, the ACO algorithm published in the literature and the NSGA-II algorithm mentioned as applied in the literature. This indicates that the system not only reduces the design cost of the building but also is able to have very good seismic performance. Moreover, due to the gradual exposure of the problems related to the seismic optimization of building structures, the technology of intelligent robotic-related systems for building structures was introduced into the effective seismic optimization of building structures, and a series of relatively modular management of seismic optimization of building structures was carried out by using subgrids for distribution. In emergency situations where both short-term high-frequency anomalies and low-frequency precursor anomalies are present, since the anomalous factors of short-term presence of high-frequency anomalies are more obvious in most cases, effective pre-processing or filtering related to the data is required to effectively detect possible anomalous low-frequency precursors.

5. Conclusion

The real-time monitoring platform for seismic optimization of building civil engineering structures is adopted to optimize the seismic structure of building civil engineering structures, which can effectively enhance the real-time monitoring ability of data. Architectural civil engineering, robotics, and structural analysis are used with seismic optimization design to improve seismic resistance. By using construction robot system technology, the creative method maximizes structural performance and seismic safety. It transforms building techniques and ensures that structures effectively endure seismic emphasis. For the constructed seismic model, starting from the data related to the surface model, accurate parameter values can be obtained. In the process of seismic dynamic monitoring, the acquired geological data is usually composed of contour lines. By comparing the structure of the model constructed on the surface, taking advantage of its complex characteristics, a small amount of drilling data information and geological section data information are used to build a geological model, and the data information that the surface model can provide can be fully utilized. The building robot system technology adopts the introduction of a good learning scheme to increase the diversity of robots. This method can be used to optimize the external file storage robot and share the optimal solution information between individuals, which improves the search speed and optimal solution. The successful calculation in practice proves the validity and feasibility of using the cluster center calculation of the building robot system in the seismic design of the building space structure. Building robot systems integration is the key to the future success of seismic optimization in civil engineering. It is possible to create robust buildings that can endure seismic disasters while reducing their negative effects on the environment and achieving the most of their resources according to this convergence of building design, construction effectiveness, and safety procedures.

6. Declarations

6.1. Author Contributions

Conceptualization, S.L. and L.S.; methodology, S.L.; software, L.S.; validation, S.L. and L.S.; formal analysis, S.L.; investigation, L.S.; resources, S.L.; data curation, L.S.; writing—original draft preparation, S.L. and L.S.; writing—review and editing, S.L.; visualization, L.S.; supervision, S.L.; project administration, L.S.; funding acquisition, S.L. All authors have read and agreed to the published version of the manuscript.

6.2. Data Availability Statement

The data presented in this study are available in the article.

6.3. Funding

The authors received no financial support for the research, authorship, and/or publication of this article.

6.4. Institutional Review Board Statement

Not applicable.

6.5. Informed Consent Statement

Not applicable.

6.6. Declaration of Competing Interest

The authors declare that they have no known competing financial interests or personal relationships that could have appeared to influence the work reported in this paper.

7. References

[1] Munteanu, R. I., Nica, G. B., Calofir, V., Iliescu, S. S., & Sirbu, O. T. (2020). Building seismic behavior improvement using an optimal control algorithm. 2020 22nd IEEE International Conference on Automation, Quality and Testing, Robotics - THETA, AQTR 2020 - Proceedings, 1–6. doi:10.1109/AQTR49680.2020.9130005.

[2] Gu, H., Liang, H., Tong, G., Liu, F., Liu, Y., Liu, X., Jia, Z., & Paul, J. (2021). Research on vibration mechanism and control technology of building structure under earthquake action. Journal of Vibroengineering, 23(6), 1395–1406. doi:10.21595/jve.2021.22090.

[3] Baghdadi, A., Heristchian, M., & Kloft, H. (2020). Design of prefabricated wall-floor building systems using meta-heuristic optimization algorithms. Automation in Construction, 114, 103156. doi:10.1016/j.autcon.2020.103156.

[4] Cerè, G., Rezgui, Y., Zhao, W., & Petri, I. (2022). Shear walls optimization in a reinforced concrete framed building for seismic risk reduction. Journal of Building Engineering, 54, 104620. doi:10.1016/j.jobe.2022.104620.

[5] Chea, C. P., Bai, Y., Pan, X., Arashpour, M., & Xie, Y. (2020). An integrated review of automation and robotic technologies for structural prefabrication and construction. Transportation Safety and Environment, 2(2), 81–96. doi:10.1093/tse/tdaa007.

[6] Leyva, H., Bojórquez, J., Bojórquez, E., Reyes-Salazar, A., Carrillo, J., & López-Almansa, F. (2021). Multi-objective seismic design of BRBs-reinforced concrete buildings using genetic algorithms. Structural and Multidisciplinary Optimization, 64(4), 2097–2112. doi:10.1007/s00158-021-02965-5.

[7] Yu, H., Peng, Z., He, Z., & Huang, C. (2023). Application maturity evaluation of building steel structure welding robotic technology based on combination weight and multi-level grey theory. Journal of Intelligent and Fuzzy Systems, 44(4), 6435–6451. doi:10.3233/JIFS-223563.

[8] Izumotani, S., Takeuchi, M., Murayama, H., & Okazaki, K. (2021). Estimating rock properties using seismic refraction survey data: a case study in an abandoned road tunnel. Exploration Geophysics, 52(4), 409–418. doi:10.1080/08123985.2020.1828856.

[9] Hao, H., Bi, K., Chen, W., Pham, T. M., & Li, J. (2023). Towards next generation design of sustainable, durable, multi-hazard resistant, resilient, and smart civil engineering structures. Engineering Structures, 277, 115477. doi:10.1016/j.engstruct.2022.115477.

[10] Goli, A., Alaghmandan, M., & Barazandeh, F. (2021). Parametric Structural Topology Optimization of High-Rise Buildings Considering Wind and Gravity Loads. Journal of Architectural Engineering, 27(4), 4021038. doi:10.1061/(asce)ae.1943-5568.0000511.

[11] Károly, L., Stan, O., & Miclea, L. (2020). Seismic model parameter optimization for building structures. Sensors (Switzerland), 20(7), 1980. doi:10.3390/s20071980.

[12] Zakian, P., & Kaveh, A. (2023). Seismic design optimization of engineering structures: a comprehensive review. Acta Mechanica, 234(4), 1305–1330. doi:10.1007/s00707-022-03470-6.

[13] Mei, L., & Wang, Q. (2021). Structural optimization in civil engineering: A literature review. Buildings, 11(2), 1–28. doi:10.3390/buildings11020066.

[14] Joyner, M. D., Gardner, C., Puentes, B., & Sasani, M. (2021). Resilience-Based seismic design of buildings through multiobjective optimization. Engineering Structures, 246, 113024. doi:10.1016/j.engstruct.2021.113024.

[15] Martin, A., & Deierlein, G. G. (2020). Structural topology optimization of tall buildings for dynamic seismic excitation using modal decomposition. Engineering Structures, 216, 110717. doi:10.1016/j.engstruct.2020.110717.

[16] Idels, O., & Lavan, O. (2021). Optimization-based seismic design of steel moment-resisting frames with nonlinear viscous dampers. Structural Control and Health Monitoring, 28(1), 2655. doi:10.1002/stc.2655.

[17] Zakian, P., & Kaveh, A. (2020). Topology optimization of shear wall structures under seismic loading. Earthquake Engineering and Engineering Vibration, 19(1), 105–116. doi:10.1007/s11803-020-0550-5.

[18] Caicedo, D., Lara-Valencia, L., Blandon, J., & Graciano, C. (2021). Seismic response of high-rise buildings through metaheuristic-based optimization using tuned mass dampers and tuned mass dampers inerter. Journal of Building Engineering, 34, 101927. doi:10.1016/j.jobe.2020.101927.

[19] Baghdadi, A., Heristchian, M., & Kloft, H. (2021). Connections placement optimization approach toward new prefabricated building systems. Engineering Structures, 233, 111648. doi:10.1016/j.engstruct.2020.111648.

[20] Ahmadie Amiri, H., & Estekanchi, H. E. (2023). Life cycle cost-based optimization framework for seismic design and target safety quantification of dual steel buildings with buckling-restrained braces. Earthquake Engineering and Structural Dynamics, 52(13), 4048–4081. doi:10.1002/eqe.3864.

[21] Baduge, S. K., Thilakarathna, S., Perera, J. S., Arashpour, M., Sharafi, P., Teodosio, B., Shringi, A., & Mendis, P. (2022). Artificial intelligence and smart vision for building and construction 4.0: Machine and deep learning methods and applications. Automation in Construction, 141, 104440. doi:10.1016/j.autcon.2022.104440.

[22] Zhang, F., Chan, A. P. C., Darko, A., Chen, Z., & Li, D. (2022). Integrated applications of building information modeling and artificial intelligence techniques in the AEC/FM industry. Automation in Construction, 139, 104289. doi:10.1016/j.autcon.2022.104289.

[23] Rane, N. L. (2023). Integrating Leading-Edge Artificial Intelligence (AI), Internet of Things (IoT), and Big Data Technologies for Smart and Sustainable Architecture, Engineering and Construction (AEC) Industry: Challenges and Future Directions. International Journal of Data Science and Big Data Analytics, 3(2), 73–95. doi:10.51483/ijdsbda.3.2.2023.73-95.